



Memorandum

To: File

From: John Effland
Dave Schmitt

Date: 2005-11-29

Revisions: 2005-11-29 jee Initial
2005-11-30 jee Minor typos
2005-11-30 jee More minor typos

Subject: Gain Stability Measurements of Band 6 Cartridge SN002

1. Summary

This memo describes measurements of gain stability for Band 6 Cartridge SN002 installed in the RAL cryostat. Gain stability was measured using a bias supply type “A” and the newer type “B”. In addition, all data were measured with a Warm Cartridge Assembly reflecting the latest production design that uses LO power amplifiers with GaAs devices rather than the InP devices.

“Appendix I: Description and Validation of Allan Variance Measurement System” on page 11 provides details on the measurement setup, Allan Variance algorithm, and the algorithm that converts from power spectral density to Allan Variance.

2. Results

Gain stability meets ALMA requirements for Band 6 Cartridge SN 002 measured at 223 GHz, 233 GHz, 243 GHz, 253 GHz and 263 GHz. Gain stability measured with both the cartridge and Front End IF switch, is the same (within measurement error) as that measured with just the cartridge. Table 1 summarizes the results.

| Table 1: Summary of Gain Stability Results, Band 6 Cartridge 002 | | |
|---|-----------------|--|
| Results | Bias Box | Notes |
| Figure 1, Figure 2, Figure 3, Figure 4, Figure 5 | 002 (Rev A) | LO ranges from 223 GHz to 263 GHz |
| Figure 6, Figure 7, Figure 8, Figure 9, Figure 10 | 005 (Rev B) | LO ranges from 223 GHz to 263 GHz |
| Figure 11, Figure 12, Figure 13, Figure 14 | 002 (Rev A) | Comparison with and without IF Switch, LO is 243 GHz and 253 GHz |

3. Acknowledgments

We wish to thank Geoff Ediss for his suggestion to use a synthesizer as a test source.

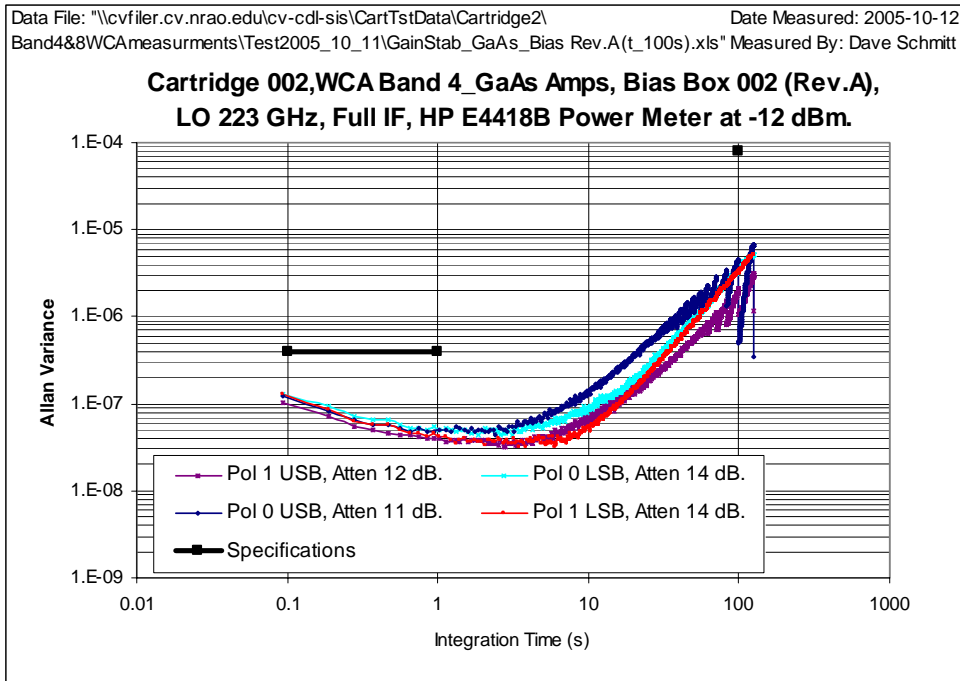


Figure 1: Allan Variance, LO = 223 GHz, Bias Supply 002 (Rev A)

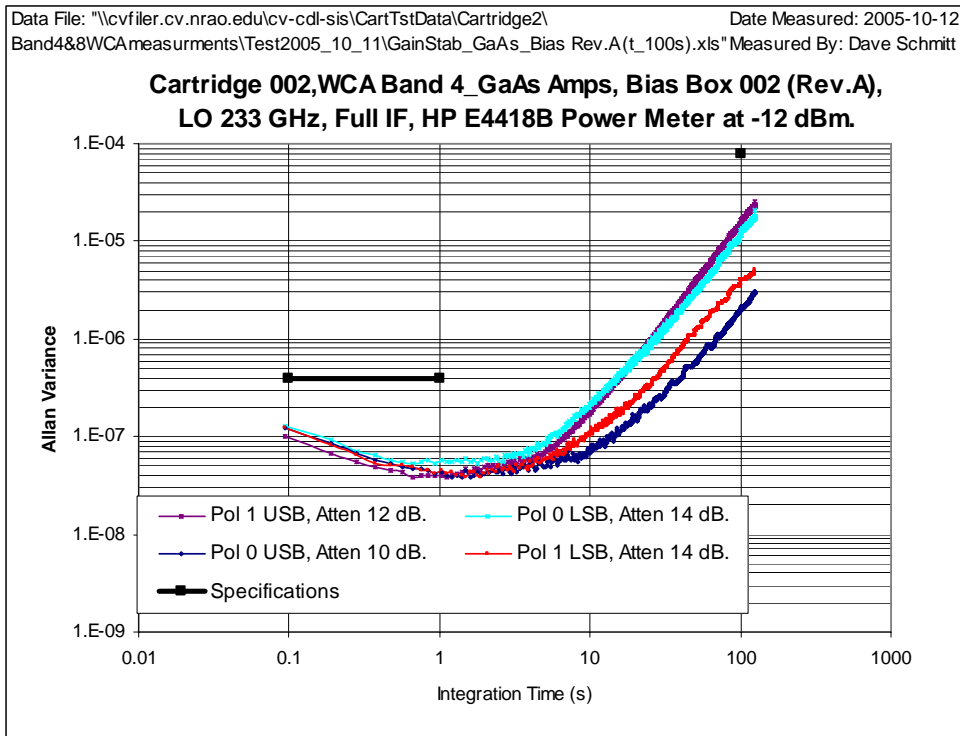


Figure 2: Allan Variance, LO - 233 GHz, Bias Supply 002 (Rev A)

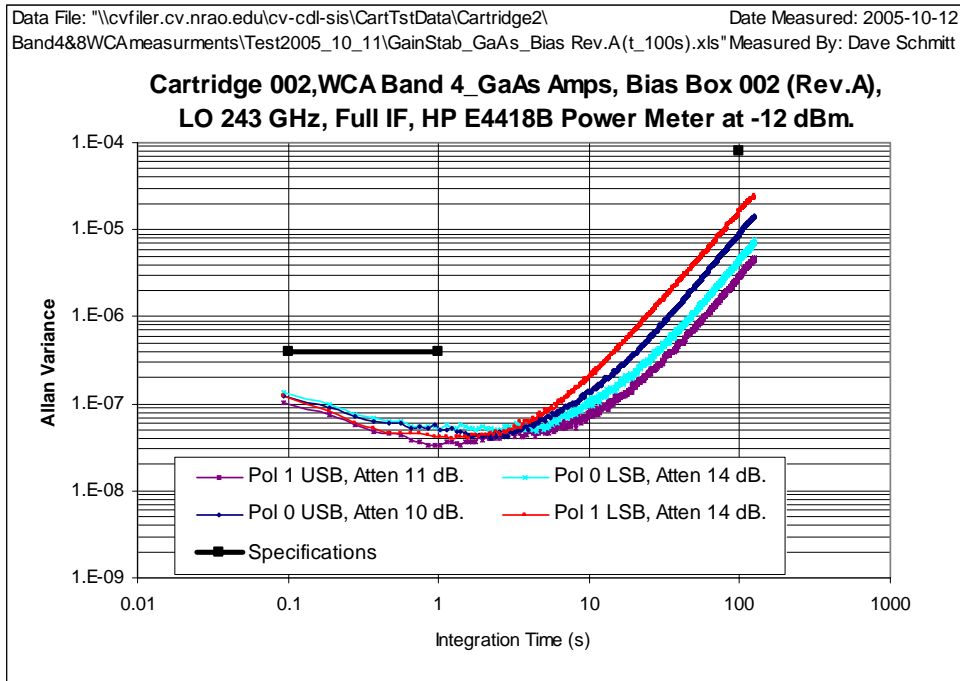


Figure 3: Allan Variance, LO = 243 GHz, Bias Supply 002 (Rev A)

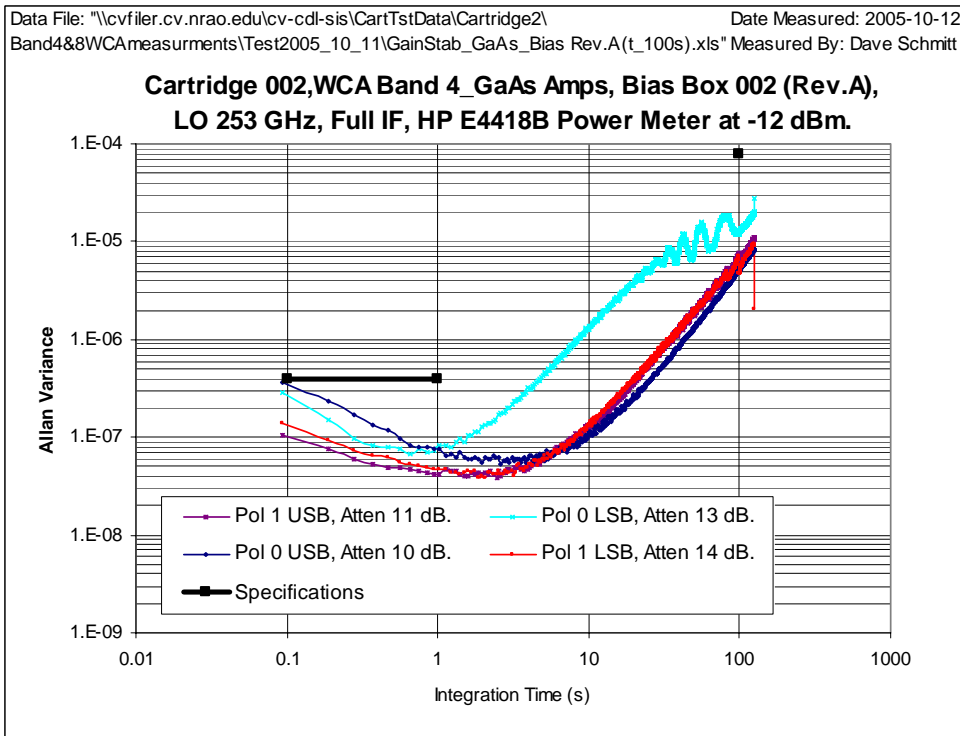


Figure 4: Allan Variance, LO = 253 GHz, Bias Supply 002 (Rev A)

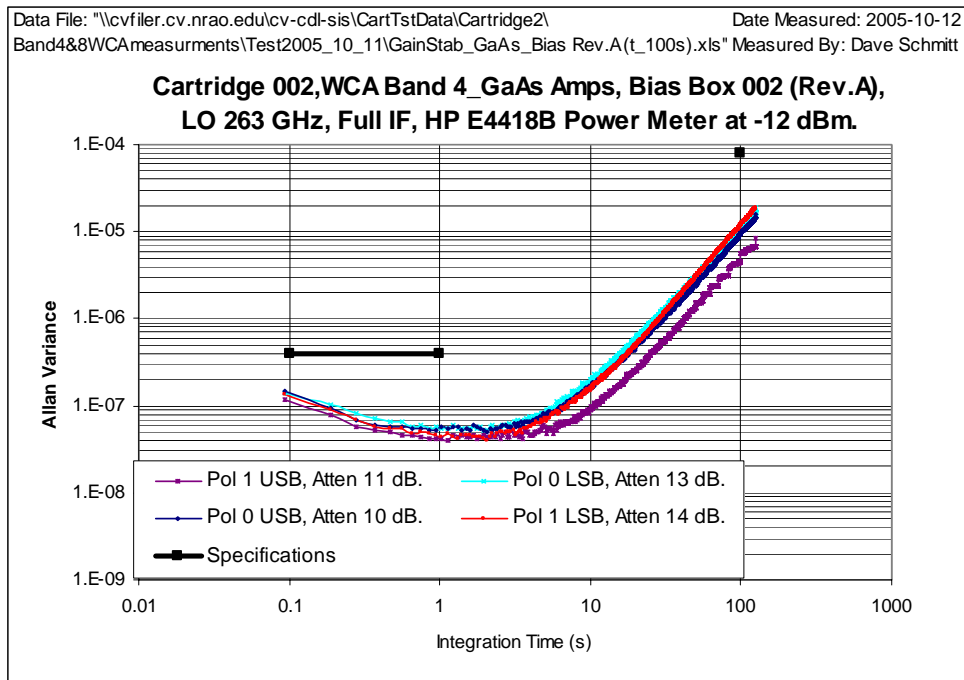


Figure 5: Allan Variance, LO = 263 GHz, Bias Supply 002 (Rev A)

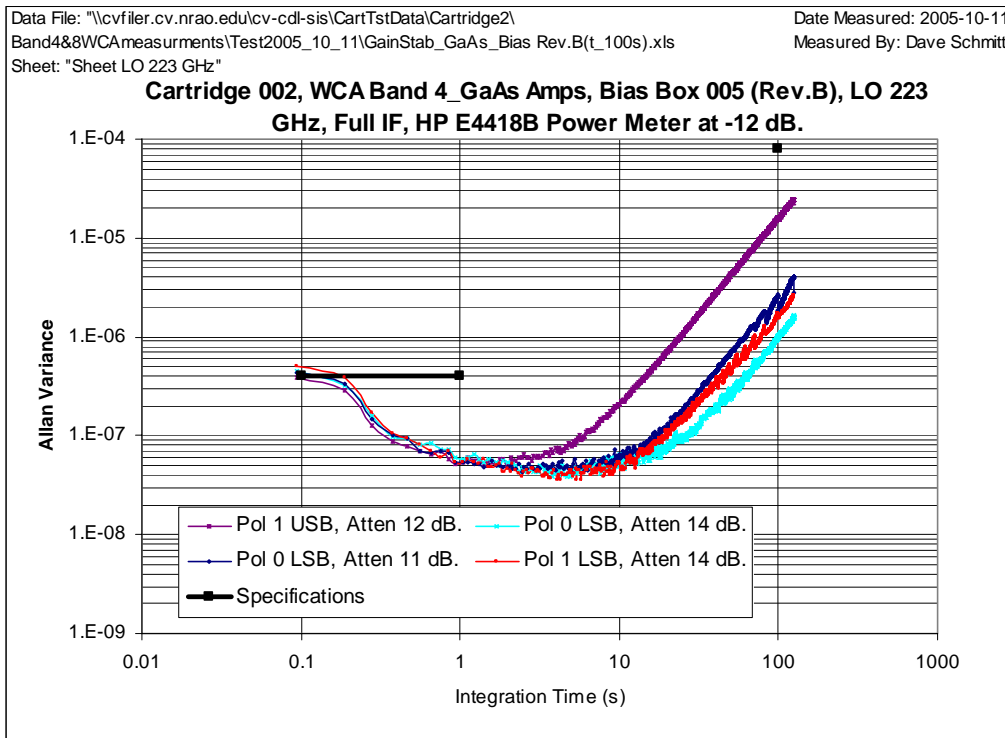


Figure 6: Allan Variance, LO = 223 GHz, Bias Supply 005 (Rev B)

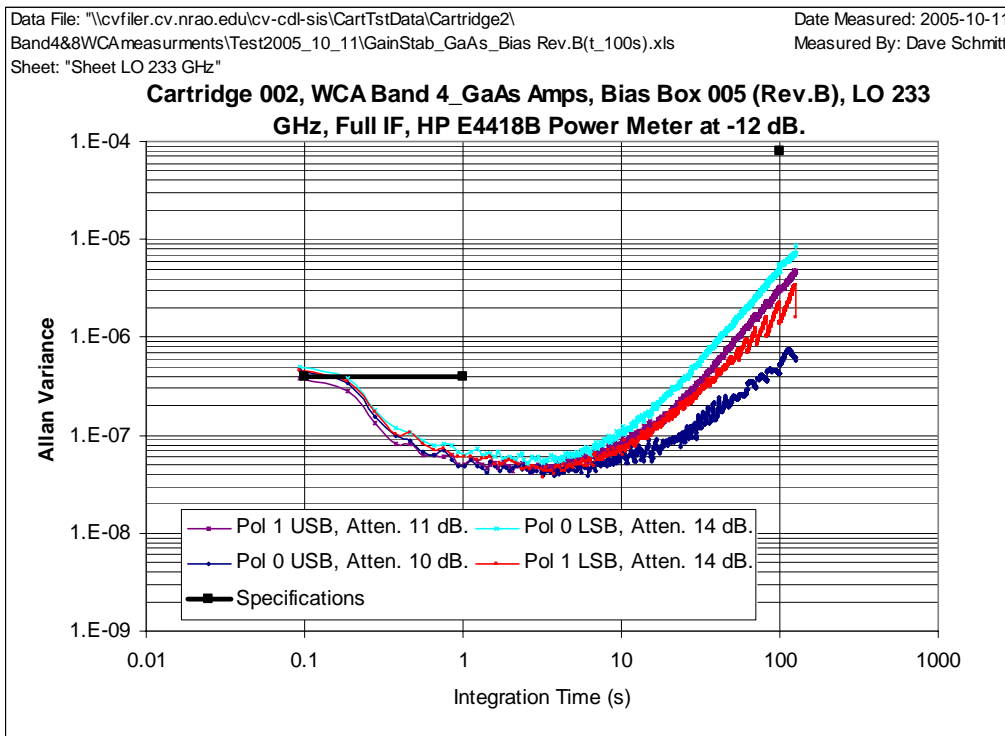


Figure 7: Allan Variance, LO = 233 GHz, Bias Supply 005 (Rev B)

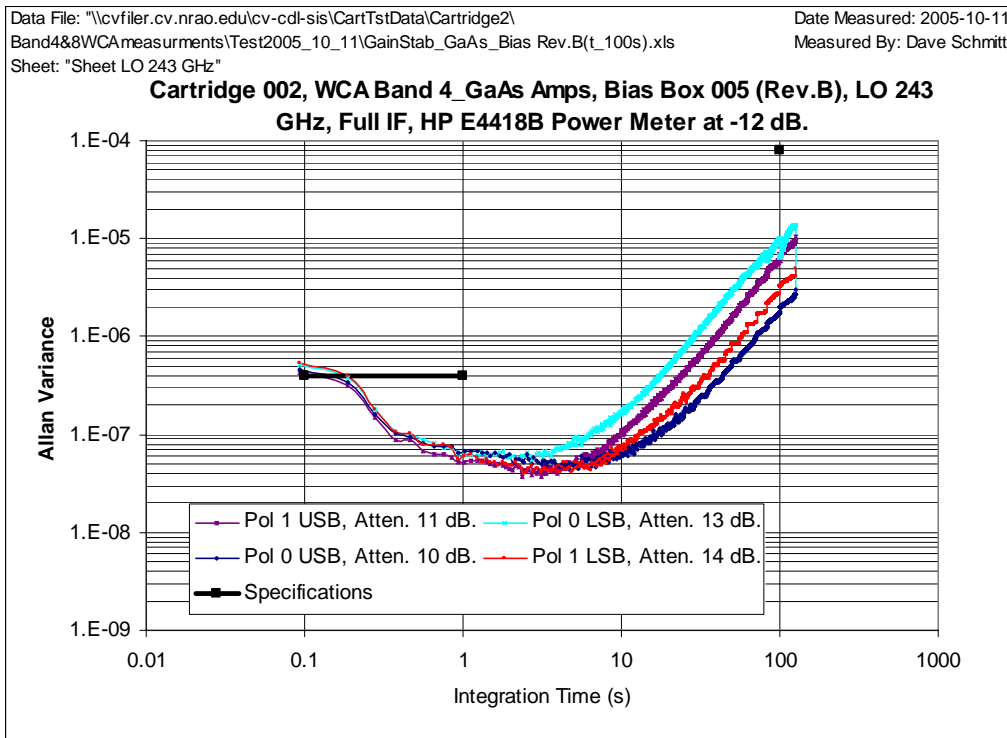


Figure 8: Allan Variance, LO = 243 GHz, Bias Supply 005 (Rev B)

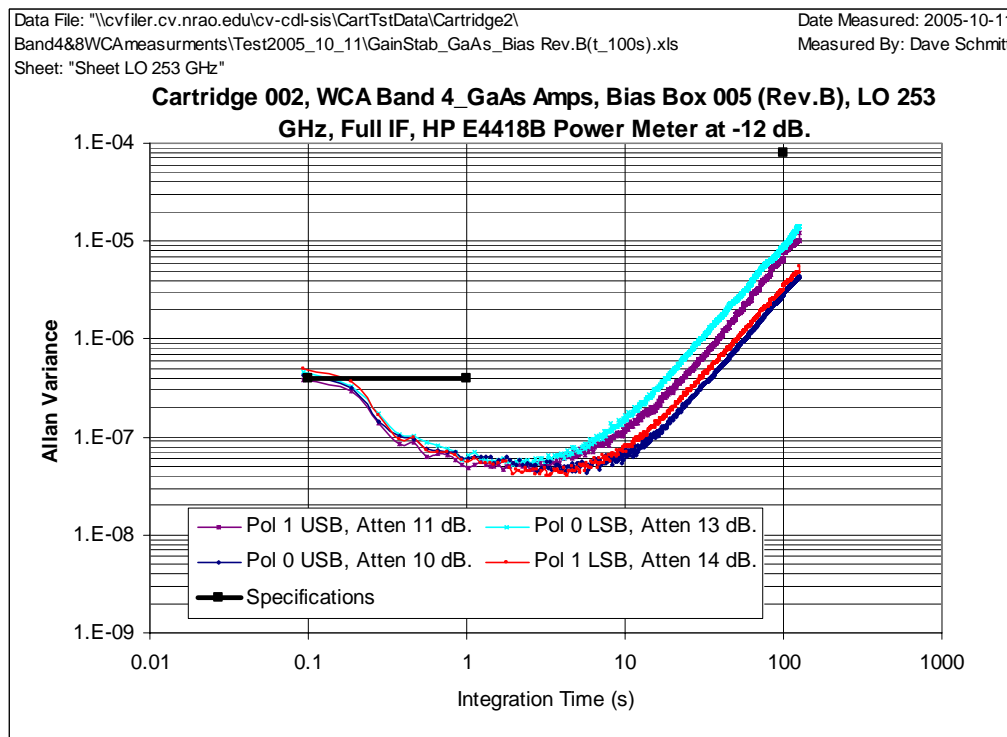


Figure 9: Allan Variance, LO = 253 GHz, Bias Supply 005 (Rev B)

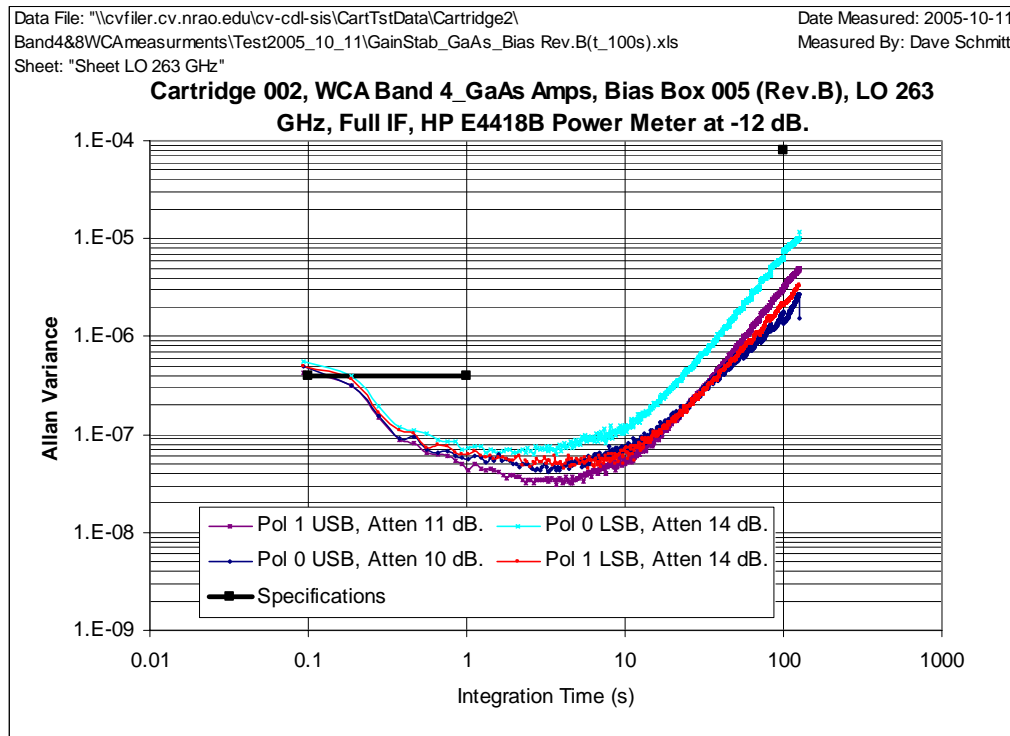


Figure 10: Allan Variance, LO = 263 GHz, Bias Supply 005 (Rev B)

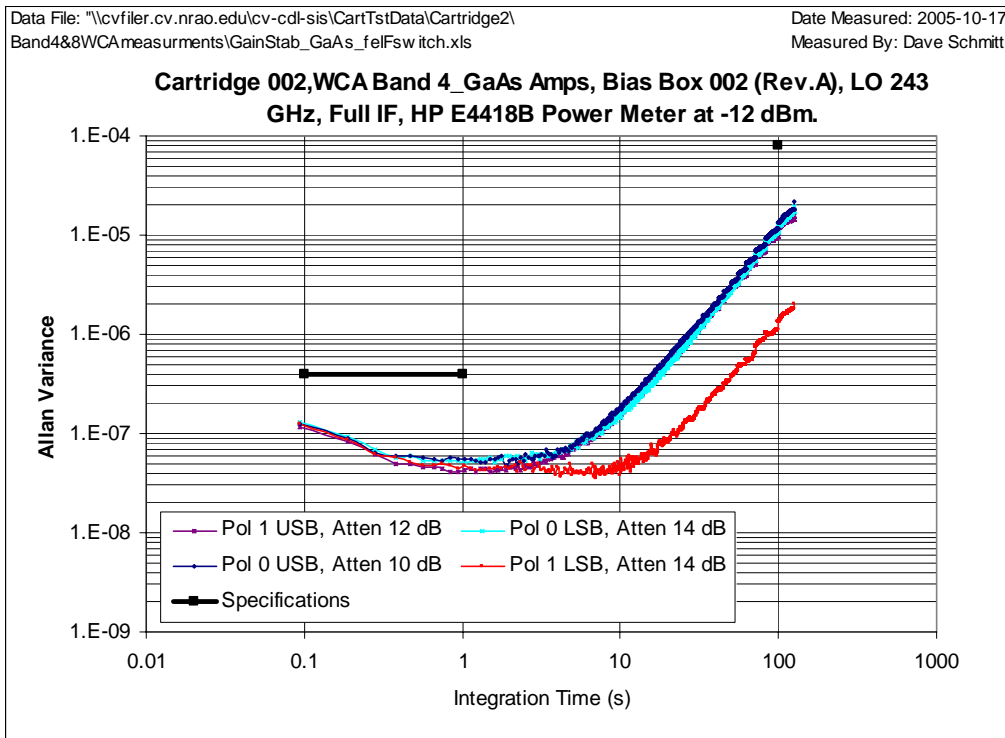


Figure 11: Gain Stability with No IF Switch, LO = 243 GHz

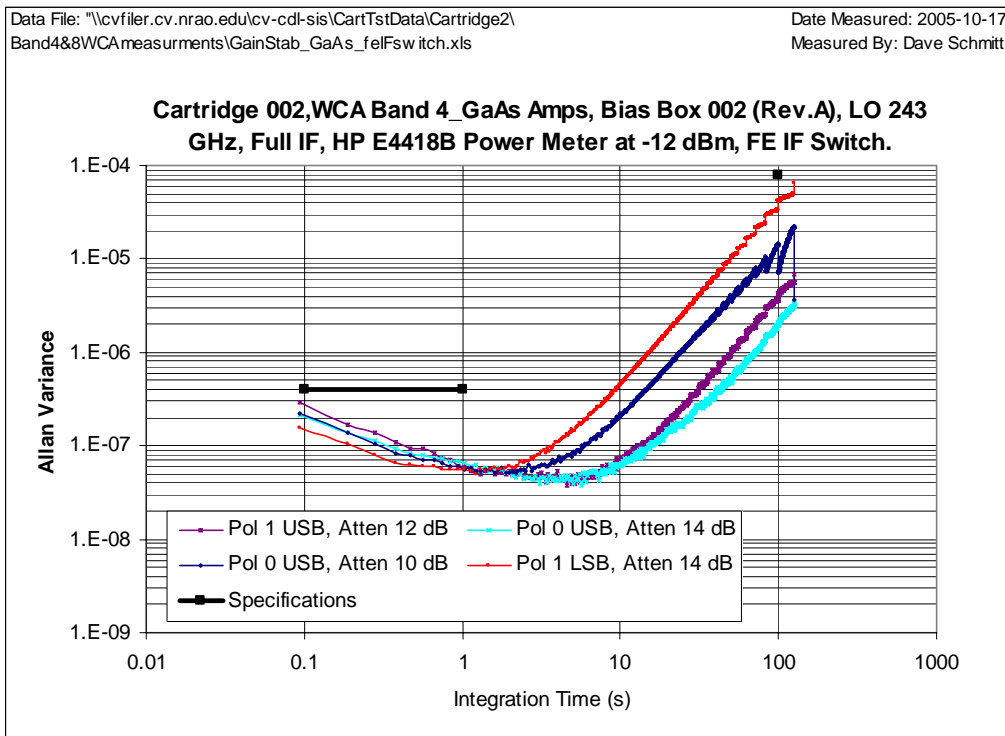


Figure 12: Gain Stability with IF Switch, LO = 243 GHz

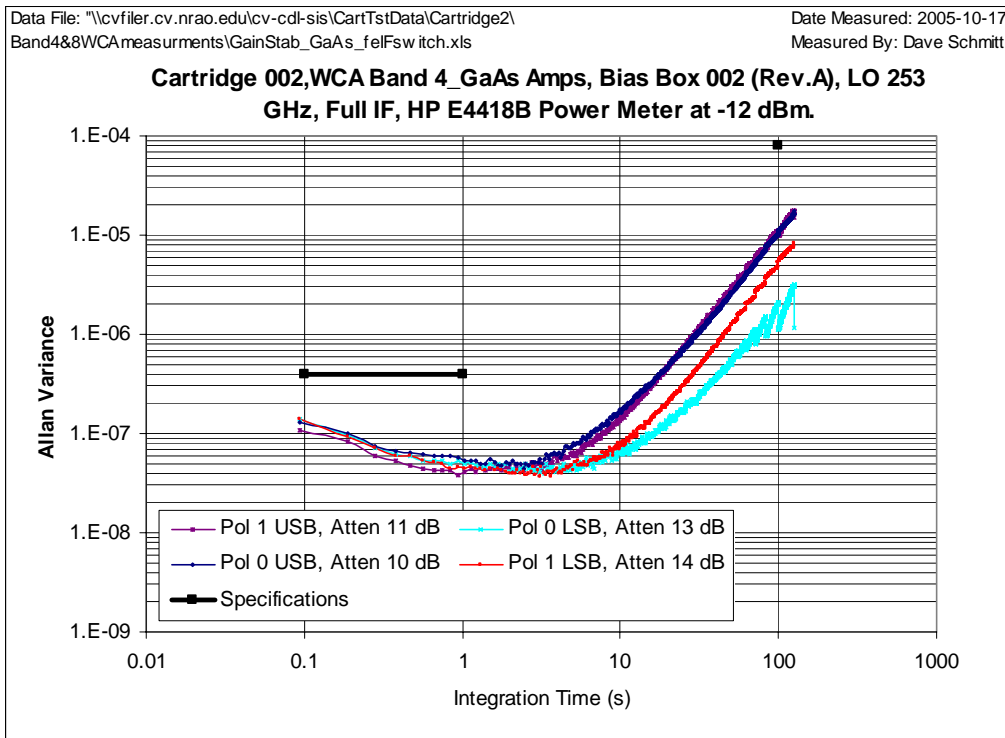


Figure 13: Gain Stability with No IF Switch, LO = 253 GHz

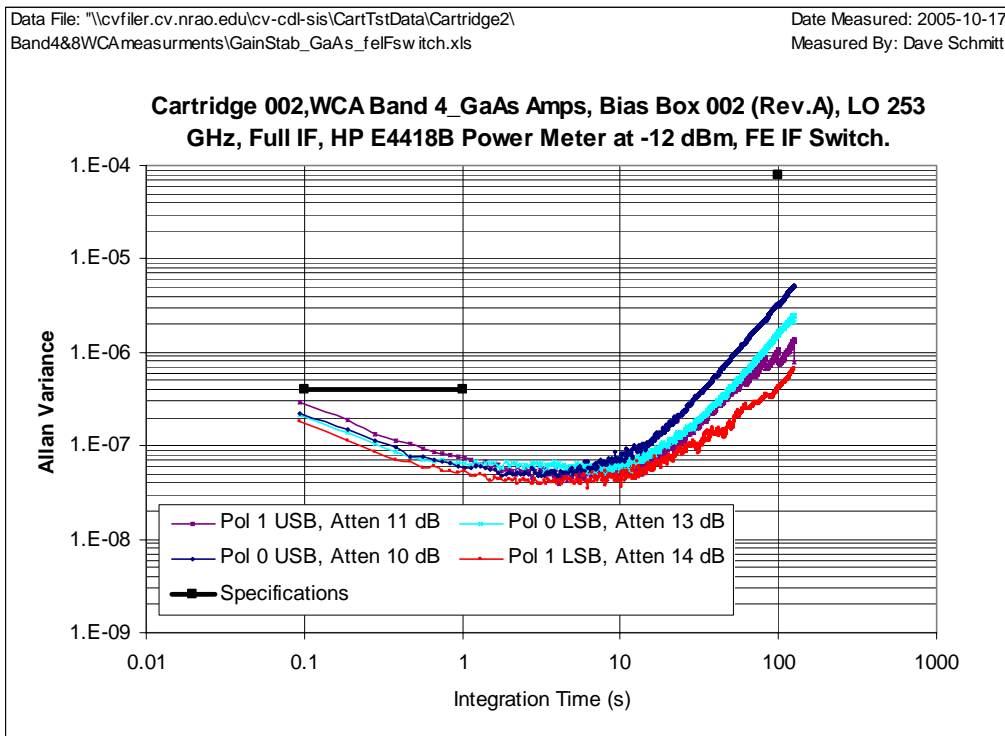


Figure 14: Gain Stability with IF Switch, LO = 253 GHz

4. Appendix I: Description and Validation of Allan Variance Measurement System

4.1 Specification

The Allan Variance specification for the Band 6 cartridge is^{1,A}

$$\sigma^2(2, T, 0.9T) \begin{cases} < 4 \times 10^{-7} & \text{for } 0.1\text{sec} < T < 1 \text{ sec} \\ < 8 \times 10^{-5} & \text{for } T = 100 \text{ sec} \end{cases}$$

where: $\sigma^2(2, T, 0.9T)$ is the Allan Variance^B, computed for a minimum of 2 samples (as specified by the first parameter),
 T is the sampling period
 0.9T is the integration time (also denoted as τ), which is 90% of the sample period, *i.e.* 10% dead time

4.2 Time Sequence to Allan Variance Algorithm

Given a sequence of power measurements, Allan Variance is computed by Excel-based software written in Visual Basic for Applications using the following equation

$$\sigma^2(\tau) = \frac{1}{2(N-1)\mu^2} \sum_{n=1}^N [v_n(\tau) - v_{n-1}(\tau)]^2$$

where: $\sigma^2(\tau)$ is the Allan Variance for an integration time (in secs) of τ ,
 μ is the mean of all the $v_n(\tau)$'s,
 N is the number of samples collected,
 $v_n(\tau)$ is the nth voltage (or power) sample after an integration time τ .

Figure 15 shows a sequence of voltage samples and how longer integration times are achieved by combining samples to reuse the single sequence of data.

The minimum integration time is achieved with the maximum sampling rate of the power meter, which is 93 ms. Although the power meter is programmed for 40 samples per second, (25 ms period), the slower sampling rate results because temperatures are measured (using a LakeShore 218 temperature meter) in the same software loop that reads the power meter.

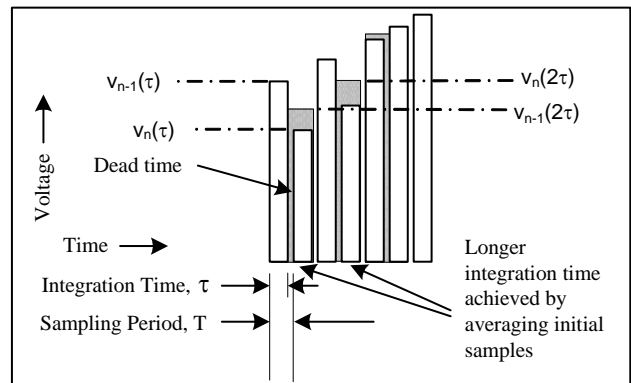


Figure 15: Time Sequence for Voltage Samples

Longer integration times are calculated by averaging samples $v_1(93 \text{ ms})$ and $v_2(93 \text{ ms})$, then $v_2(93 \text{ ms})$ and $v_3(93 \text{ ms})$, and so on. Although ALMA specifications allow for only two samples to be averaged when calculating

¹ References are denoted with letters and are given at the end of this section, page 26.

the Allan Variance for the longest integration time, empirical studies show the variance of the result is excessive when averaging such a small number of samples, so the software requires at least 4 samples to compute the maximum averaging time.

The software that computes Allan Variance from the time sequence of power measurements was validated by computing gain stability for a normally-distributed, 30,000 point sequence with $\sigma = 0.001$ and $\mu = 1$ generated from Excel's Data Analysis Toolpack. Figure 16 shows the output of the Allan Variance routine for this case. An arbitrary rate of 10 measurements per second (0.1s integration time) was assumed for the Excel-generated data. Note the Allan Variance shows the correct value of 1.0×10^{-6} at an integration time of 0.1s and the slope of the line is 1:1. Uncertainty increases as the number of samples for averaging decreases, and such uncertainty is evident for long integration times in Figure 16.

The current version of the software, written in Visual Basic for Applications, is stored in Excel spreadsheet files and Table 2 lists the major software routines used.

4.3 Hardware

Two different hardware configurations were used as power detectors to measure Allan Variance with time sequences and the results are quite similar. The "Power Meter System" consisted of an Agilent 4418B Power Meter with E9300A power head and was configured by the software to take 40 readings per second with no averaging. Although this power meter can achieve 200 measurements per second, experiments showed that, for the same integration time, the Allan Variance was worse by a factor of 10 when used in the highest speed mode.

The second power detector was a "Tunnel Diode System" consisting of a 3 dB attenuator, an HP8473B tunnel diode detector, a Stanford Research SR560 Video Amp set to a gain of 50, and an HP 34401A DVM. Figure 19 is the measured linearity of the entire measurement system chain when using the tunnel diode and shows that detector system remains linear to a power level around -10 dBm.

Figure 18 is a block diagram of the equipment used for gain stability measurements. Gain stability was measured over the entire IF range from 4 – 12 GHz with a 4 GHz high pass filter employed to reduce noise power below the IF band but no filtering was used above 12 GHz.

To validate both power detection systems, Allan Variance was measured with each by replacing the noise power from the cartridge with the output from an HP 8341B synthesizer. The Allan Variance as a function of power level for both tunnel diode and power meter detectors is shown in Figure 20 and Figure 21 when using the synthesizer as a source. Power data vs. time with the synthesizer as a source for both detector types is graphed in Figure 22 and Figure 23. Long-term drift is readily apparent in the tunnel diode detector data, Figure 23 and consequently in the Allan Variance plot of Figure 21. Although the tunnel diode detector system has better short-term Allan Variance (Figure 21), the power meter exhibits better long-term stability, as shown in Figure 20. Consequently, the power meter was used for most Allan Variance measurements.

To compare both detector systems, the input power was set for the optimum value for each detector type: -12 dBm for the tunnel diode system and -17 dBm for the power head. Figure 24 compares gain stability measurements of the cartridge at 233 GHz using both detector systems and shows very close agreements for integration times from 0.1s to 1s. Long-term drift differs for both types of detectors, but that's not surprising given the temperature dependant long-term stability characteristics of the receiver.

4.4 Conversion from Power Spectral Density to Allan Variance

The HP 35670A Dynamic Signal Analyzer provides another means for collecting gain stability data and has the added advantage of showing directly gain fluctuations from refrigerator effects and power-line contamination. Figure 25 shows measurements from the Dynamic Signal Analyzer after converting the data from spectral density, as given in units of V_{rms} per root-Hertz, to fractional gain stability obtained by dividing the spectral density by the DC (or mean) voltage^C. The results in Figure 25 were measured at the input to the “E4408 Spectrum Analyzer,” shown in the block diagram of Figure 18, and include contributions from the second amplifier on the warm IF plate. The spectrum of the IF as seen by the tunnel diode detector is shown in Figure 26. The data in this Section 4.4 is intended to validate the software routines and should not be compared to the actual gain stability data in the main body of the report.

The normalized power spectral density (PSD) data shown in Figure 25 is obtained by concatenating a series of PSD measurements obtained sequentially from the HP 35670A. Each individual series consists of 1600 points measured with maximum frequencies of 102 kHz, 12.8 kHz, 1.6 kHz, and 100 Hz and each series is indicated by different colors in Figure 25.

The point in Figure 25 denoted “SQRT(2/8 GHz)” shows the limiting case when the PSD should approach root 2 over the pre-detection bandwidth^D. The measured data indeed overlaps the theoretical point and validates the PSD results.

Figure 27 is the time sample data obtained from the HP 35670A and was used by that instrument to calculate the 100 Hz max frequency PSD data presented in Figure 25.

A one-to-one conversion from PSD to Allan Variance exists^{E,F,G} and can be shown algorithmically as

$$\sigma^2(\tau) = 2 \sum_{n=2}^N PSD_n \frac{\sin^4(\pi\tau f_{n,bin})}{(\pi\tau f_{n,bin})^2} f_{step}$$

| | | |
|--------|------------------|--|
| where: | $\sigma^2(\tau)$ | is the Allan Variance for an integration time (in secs) of τ , |
| | N | is the number of FFT samples collected, |
| | PSD _n | is the normalized power spectral density obtained by dividing the amplitude in the n th FFT bin (in units of V_{rms}/Rt -Hz) by the DC voltage, |
| | $f_{n,bin}$ | is the frequency (Hz) of the n th bin, and |
| | f_{step} | is the bin width in Hz, assumed the same as the bin width, which in fact is constant and not a function of n. |

Note that the summation starts with the second, non-zero frequency bin. Also, when the argument of the sine is a multiple of π , the kernel and hence the summation is ideally zero. This degeneracy point appears to be ignored in the literature and has been deleted from the data presented below. In addition, points where the argument approaches the value of π suffer from large conversion errors, as will be discussed later.

Figure 28 compares results from two independent software routines; one that converts PSD to Allan Variance and the other that converts time sequences to Allan Variance. The original time sequence data, shown in Figure 27, was converted to Allan Variance and labeled as the “From Time Samples” curve in Figure 28. The original PSD data, shown in Figure 25, was converted to Allan Variance and is plotted as the “From FFT Data” curve in Figure 28. Both curves overlap closely from 0.01 s to 0.1 s, but diverge by about a suspicious factor of $\sqrt{2}$ from 0.1 s to 1 s. The cause of this discrepancy, which is modest given other uncertainties in measuring Allan Variance, is under investigation.

An anomaly in the algorithm occurs when the HP 35670A returns the lowest frequency bin for each series. The argument of the sine factor for that bin is a multiple of π , so the summation approaches zero. While that singularity has been deleted from the data, nearby points also show some error, as seen by the general amplitude reduction in the data for the longest integration times.

Figure 29 shows Allan Variance as calculated from the sequence of PSD measurements available directly from the HP 35670A and presented in Figure 25. It is interesting to compare measured results shown in Figure 29 to the theoretical Allan Variance of Figure 17 which includes a superimposed sine wave with 100 second period. The measured results of Figure 29 show similar ripple at short integration times, with the first null at 17 ms, which is the period of the 60 Hz sine wave shown in Figure 25.

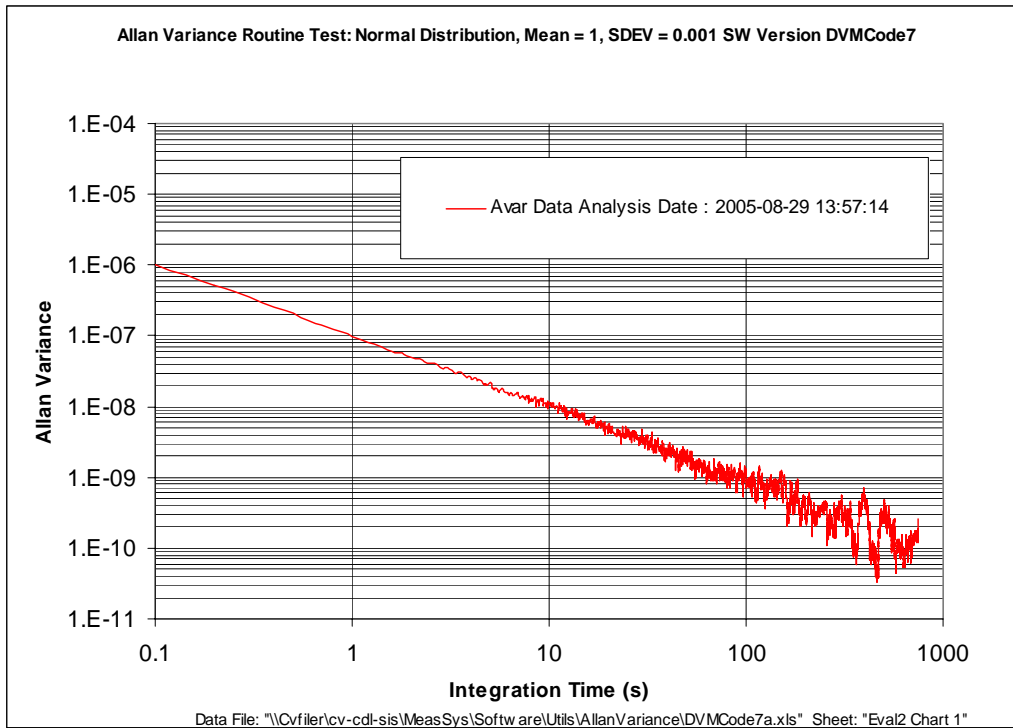


Figure 16: Validation of Allan Variance Software:
 Input is 30,000 point sequence, normally distributed, with $\sigma = 0.001$ and $\mu = 1.0$

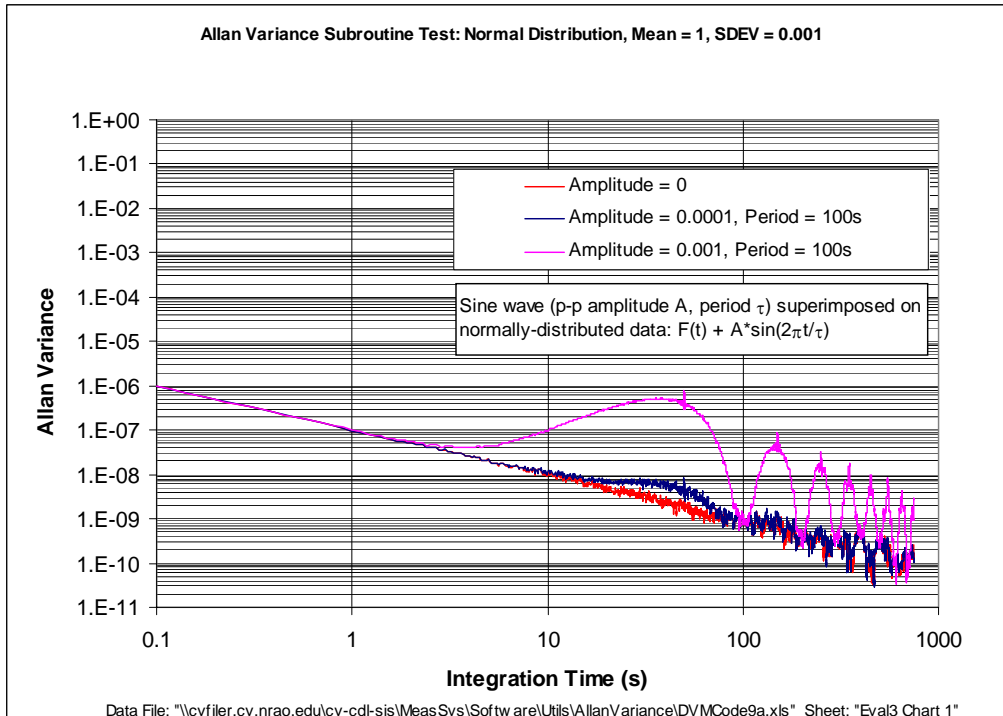


Figure 17: Simulated data of Figure 16 with superimposed sine waves

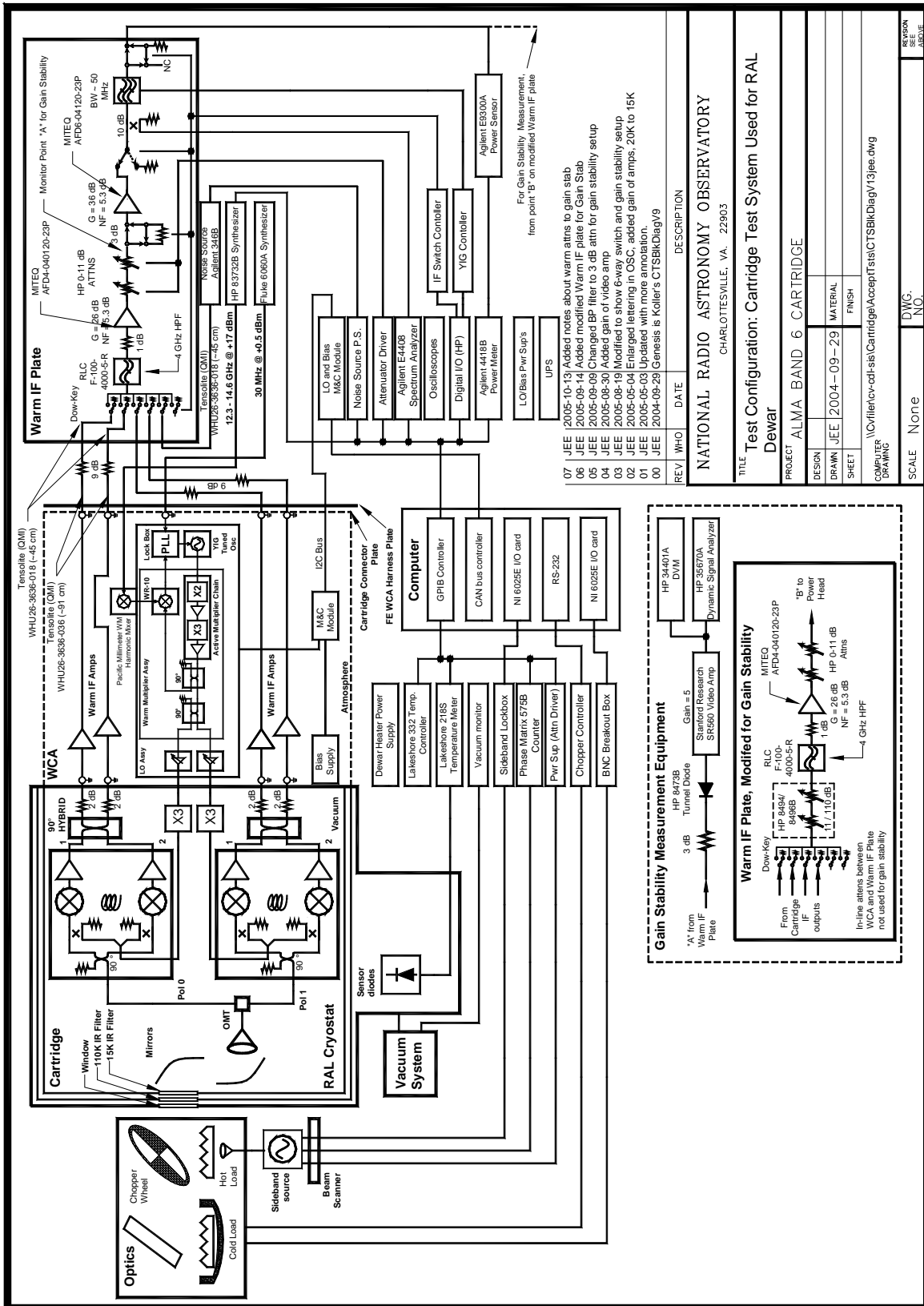


Figure 18: Measurement System Block Diagram

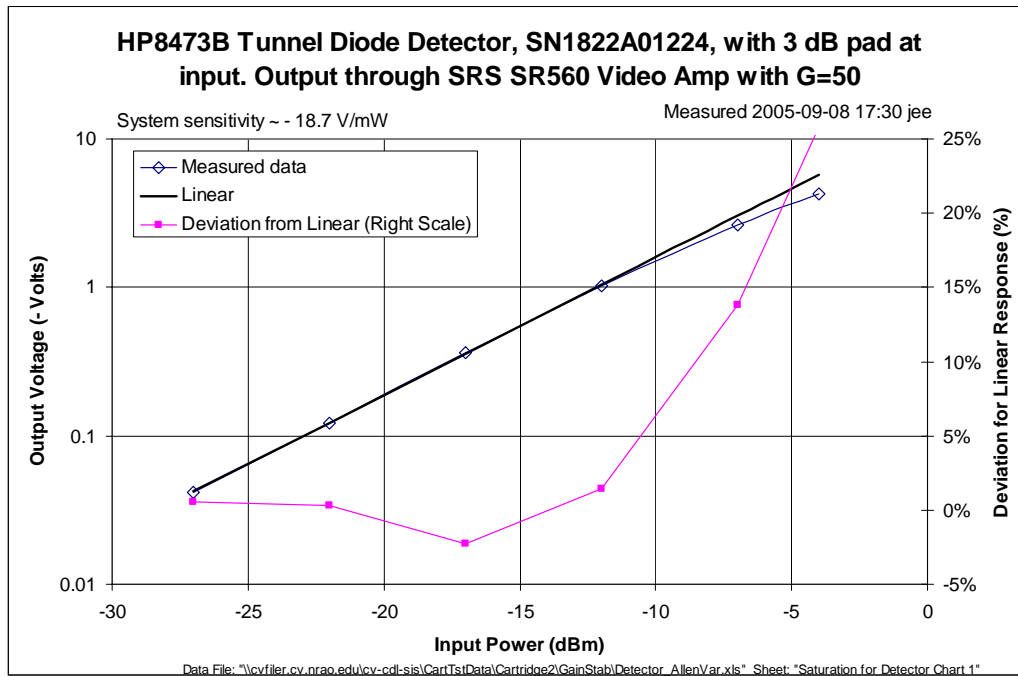


Figure 19: Linearity of measurement system with HP8473B Tunnel Diode Detector

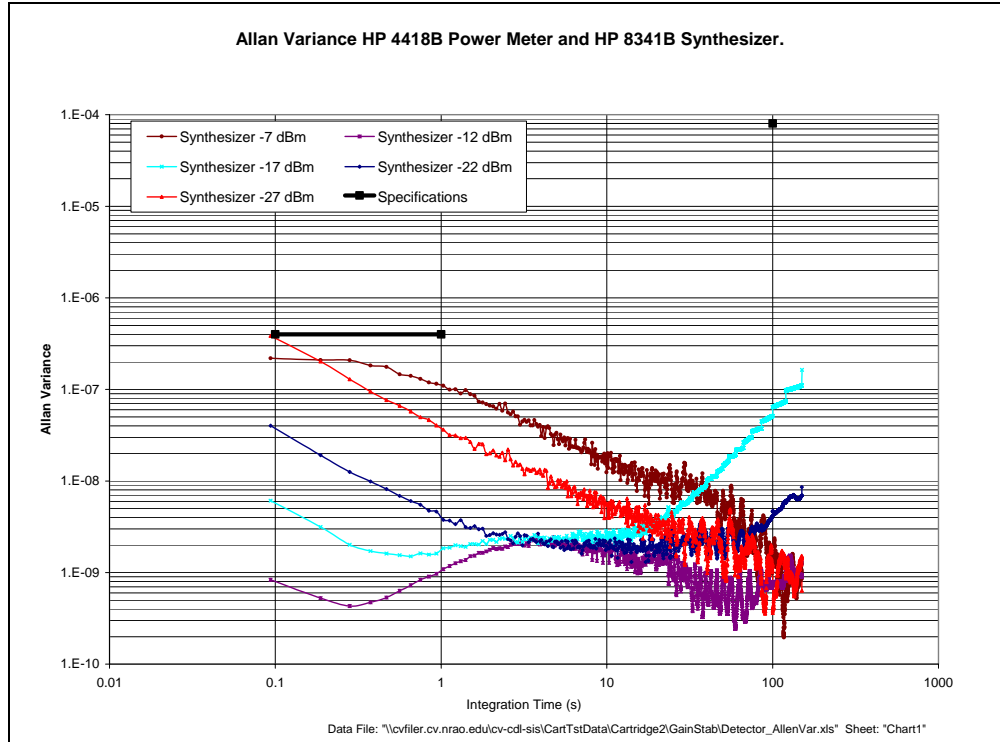


Figure 20: Allan Variance with Synthesizer as Source using Power Meter as detector

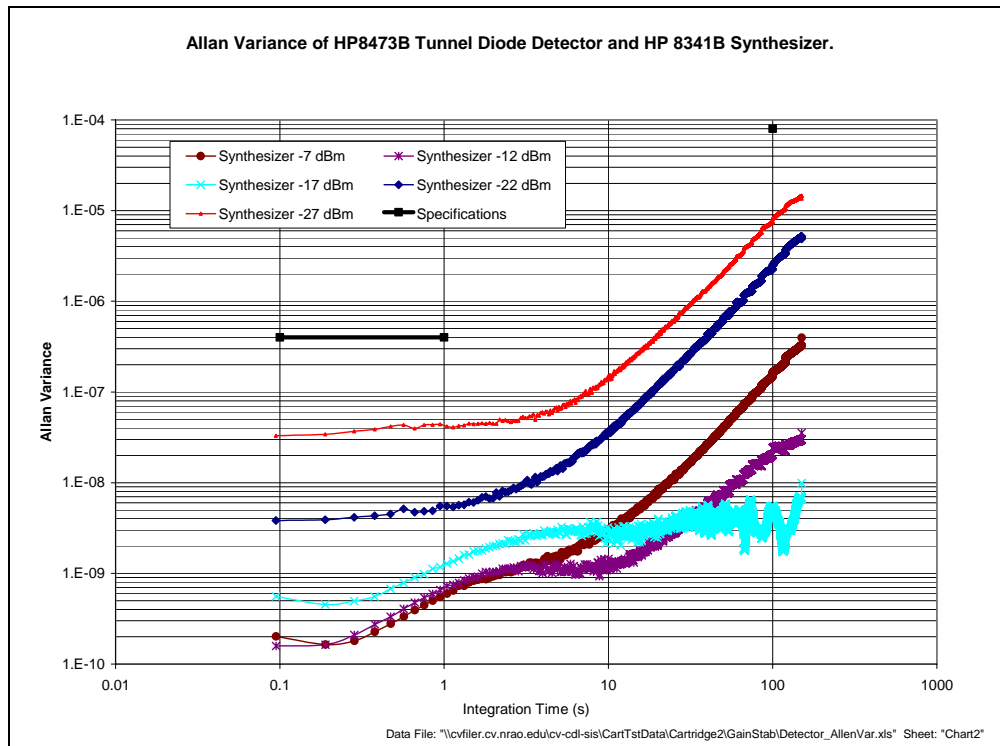


Figure 21: Allan Variance with Synthesizer as Source using HP8473B Tunnel Diode as detector

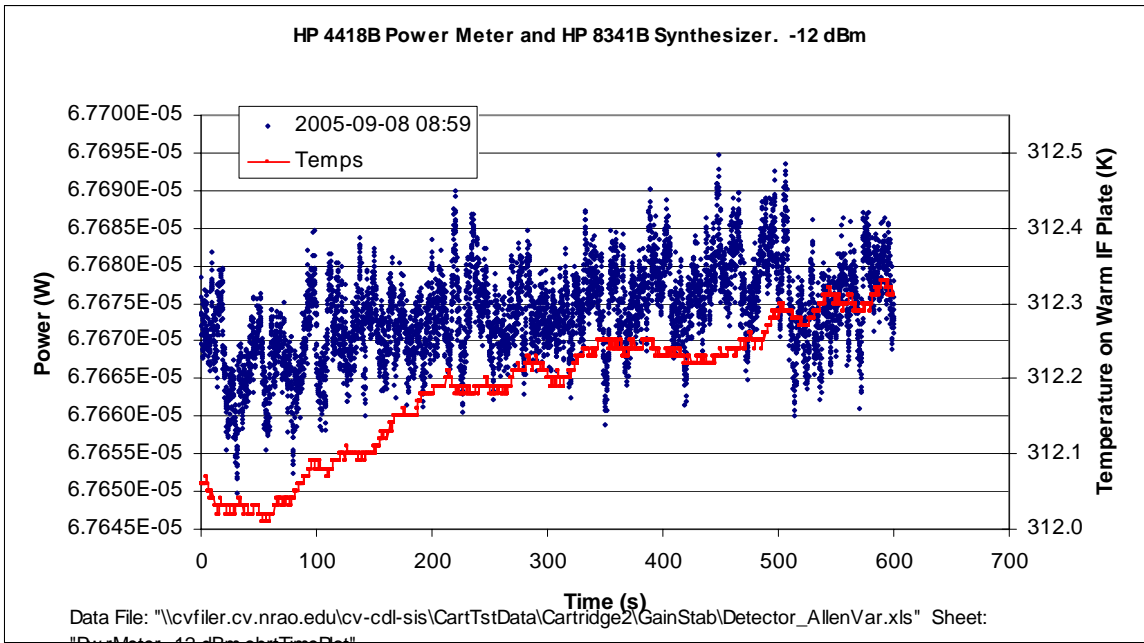


Figure 22: Time series for “Synthesizer -12 dBm” curve in Power Meter Avar, Figure 20

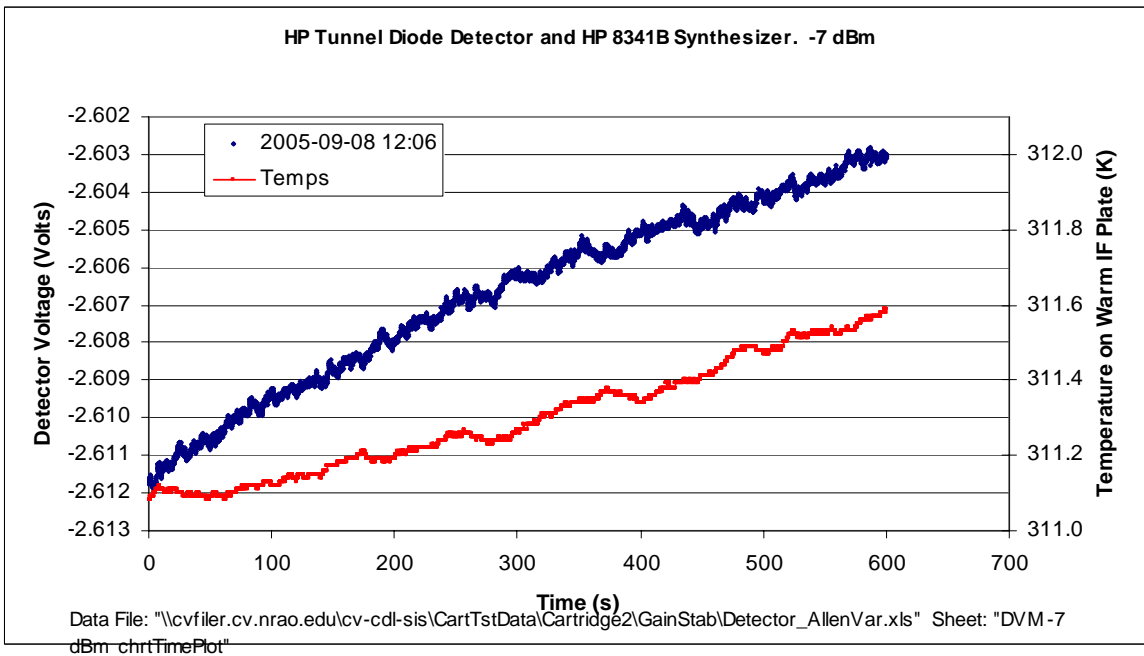


Figure 23: Time Series for “Synthesizer -7 dBm” curve Tunnel Diode Avar in Figure 21

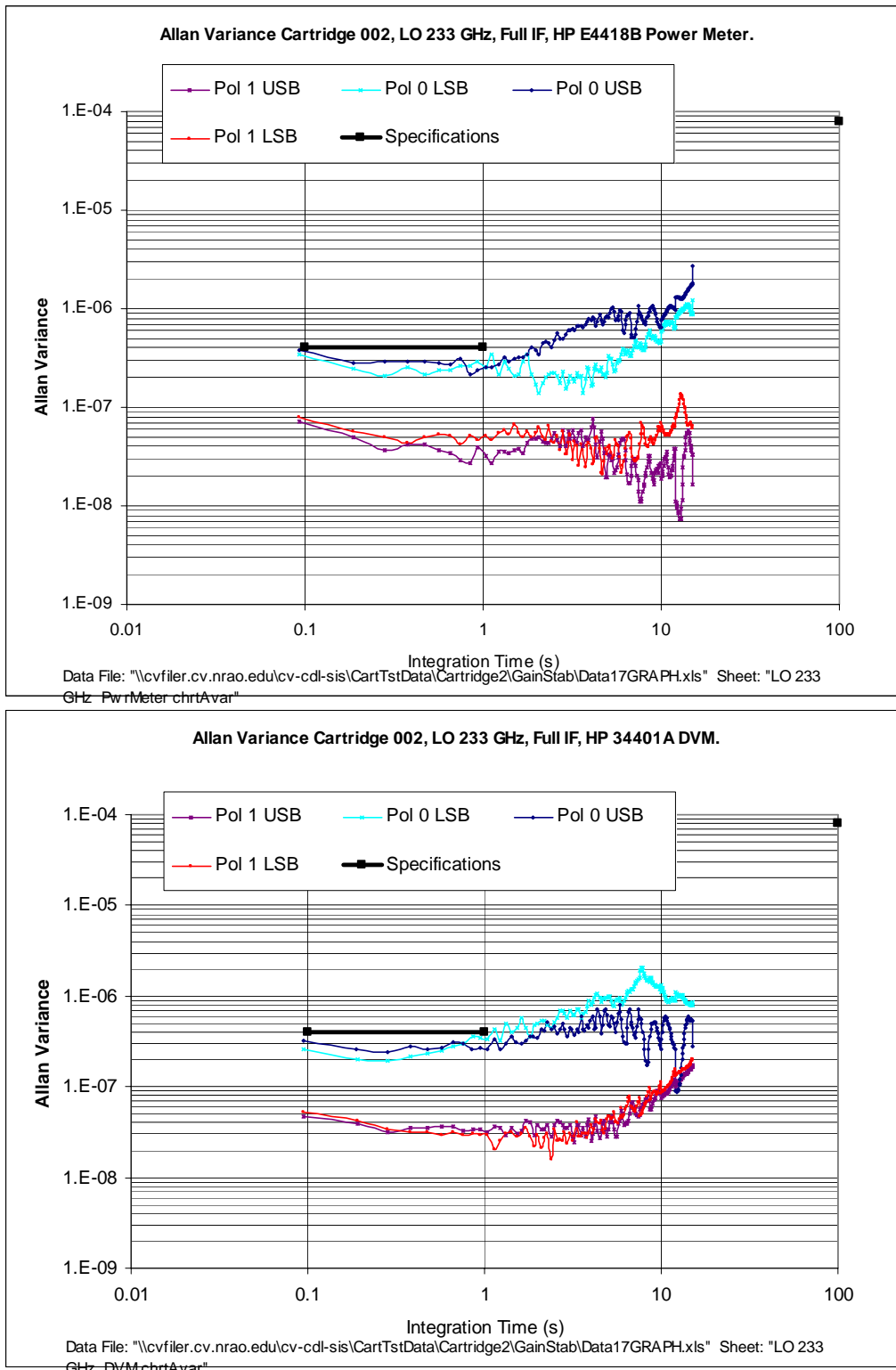


Figure 24: 233 GHz, Allan Variance measured with Power Meter (Upper Graph) and Tunnel Diode Detector (Lower Graph). Data were measured with Bias Box 005 prior to repair of channel 0 that caused unusually poor gain stability.

| Table 2: Software Routines in \\cvfiler.cv.nrao.edu\cv-cdl-sis\MeasSys\Software\Utils\AllanVariance\DVMCode9a.xls | | |
|--|----------|---|
| Routine | Module | Description |
| Sub SetUpMenus() | Utils | <ul style="list-style-type: none"> • Builds the menu Avar and displays it in Excel with the following submenus: • Get Data and Graph – collects the data and graphs it, all to a new worksheet. • Acquire Data – collects the power and temperature data, stores it on a new worksheet • Computer Avar – computes the Allen Variance from data on the active Excel worksheet. The power data must be selected, and the first cell of the selection should be the time spacing between samples, with subsequent cells the power meter readings • About – gives the current software version |
| Sub GetAndComputeAvar(ByVal nTimeInteg As Single, ByVal mtrType As mtrType, Optional ByVal sTitle As String = "") | Acquire | Copies the template sheet from the code file to the active Excel file, reads the power meter and temperature sensor, places the results on the template, computes the Allan Variance from the power meter data, and finally graphs the time and Allan Variance results. nTimeInteg is maximum integration time, mtrType represents either power meter or the HP3440 DVM, and sTitle is the title of the graph. |
| Function bGetAverageArray(ByVal lNumPtsAvg As Long, ByRef ardVolts() As Double, ByRef ardVoltsAvg() As Double) As Boolean | Analysis | Generates an average array ardVoltsAvg where each element is the average of every lNumPtsAvg elements in the input array ardVolts. |
| Sub CopyAvarTemplateSheet(ByRef sNameSheet As String) | Utils | Copies the template sheet from the add-in workbook to the active workbook. The template includes time and Avar graphs. |
| Sub ReadMeter(ByVal mtMeterType As mtrType, ByVal nTimeInteg As Single, ByVal sSheetName As String) | Acquire | Reads either the power meter or DVM (determined by mtMeterType) for nTimeInteg (parameter sSheetName is not used) and stores the time from start, reading, and temperature to columns in the active sheet. |
| Sub GraphTimeData(ByVal rngXData As Range, ByVal rngYDataPwr As Range, ByVal rngLabelPwr As Range, ByVal rngYDataTemp As Range, ByVal rngLabelTemp As Range) | Utils | Generates the power level vs. time graph by updating the graph on the template. Abscissa data in spreadsheet range specified by rngXData, ordinate values in range rngYDataPwr, label for power data is in range rngLabelPwr, temperature data in spreadsheet range rngYDataTemp, and label for temperature data is in range rngLabelTemp. |

| Table 2: Software Routines in \\cvfiler.cv.nrao.edu\cv-cdl-sis\MeasSys\Software\Utils\AllanVariance\DVMCode9a.xls | | |
|---|---------------|---|
| Routine | Module | Description |
| Sub GraphAvarData(ByVal rngXData As Range, ByVal rngYData As Range, ByVal rngYLabel As Range) | Utils | Generates the Allan Variance graph by updating the graph on the template. Abscissa data in spreadsheet range specified by rngXData, ordinate values in range rngYData, label for data is in range rngYLabel |

| Table 3: Software Routines in \\cvfiler.cv.nrao.edu\cv-cdl-sis\MeasSys\Software\Utils\AllanVariance\Code18.xls | | |
|--|--|---|
| Routine | Module | Description |
| Sub AvarFromFFT() | AVAR | Calculates the Allan Variance from the selected column of FFT values |
| Sub MeasureFrequencySet() | Read35670A | Takes a series of PSD measurements with each max frequency provided in array sFreqs() |
| Sub ReadTrace() | Read35670A | <ul style="list-style-type: none"> Reads the active trace from the HP 35670A Dynamic Signal Analyzer and places the freq and amplitude results in the next two empty rows. Also assumes a chart is available and adds the latest data to the chart. The cell in row 1 just above the transformed amplitude data is mapped by this program into the name of the data. |
| Function bNormalizedAmps(ByVal dFreqStep As Double, ByRef arAmps() As Double, ByRef arNormAmps() As Double) | Read35670A | <ul style="list-style-type: none"> Uses the frequency step in Hz dFreqStep and PSD bin values arAmps (in $V_{rms}/rtHz$) to generate V_{rms}/Vdc data as array arNormAmps() 'NOTE: THIS ASSUMES UNIFORM WINDOW (HANNING WINDOW REQUIRES: $dZeroFreqAmps * Sqr(3\# * dFreqStep)/2\#$!!!) |
| Class CGPIB() | SIS Instrument Interface 2003-10-01 V5.2.71 ² | This is the general GPIB class for communicating with the HP 35670A and written in stand-alone Visual Basic Version 6 and referenced via an "ActiveX" DLL library. |
| Function ArrayFromDelimitedString(ByVal sInputBuff As String, ByRef arValues() As Double) | Read35670A | Creates an array of values from a comma-delimited string sInputBuff and places the results in the output array arPowers. Used to parse the string returned from the HP 35670A. |

² "SIS Instrument Interface" is an ActiveX DLL located at \\cvfiler\cv-cdl-sis\MeasSys\Software\ExcelIntf2p94\lib5.2.71.dll

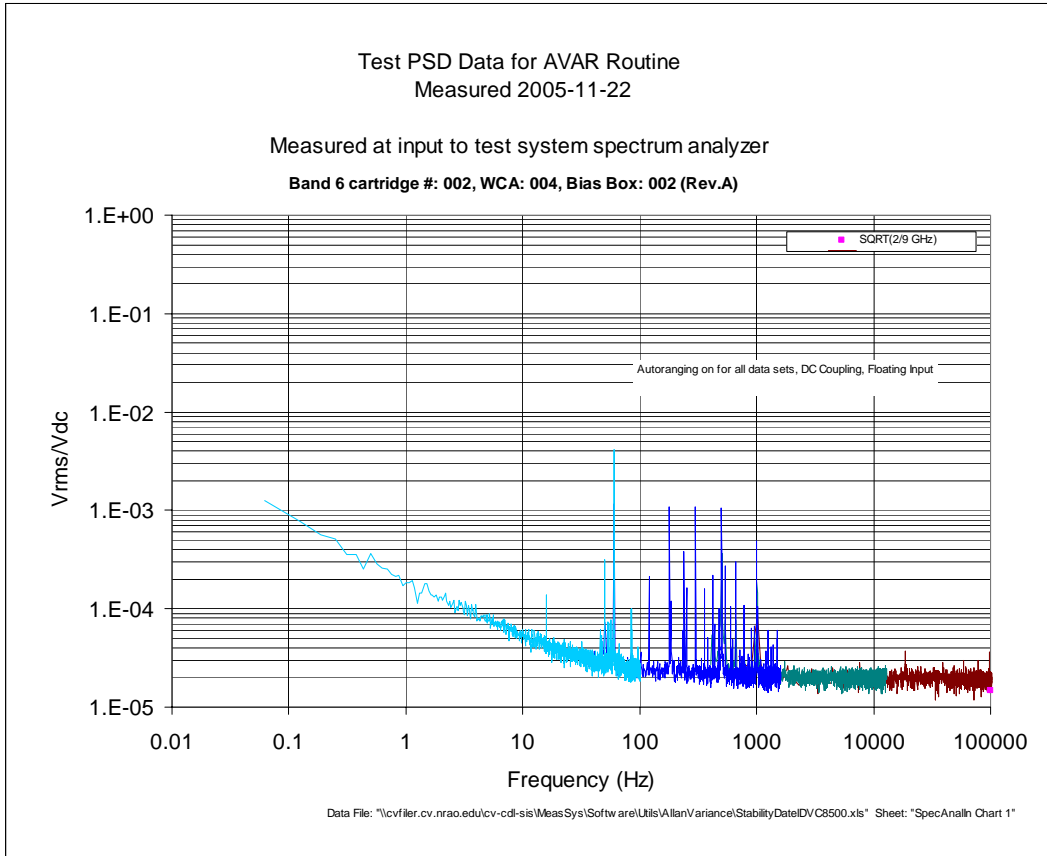


Figure 25: PSD Data used to test conversion from PSD to AVAR



Figure 26: IF Spectrum Measured using HP 35670A

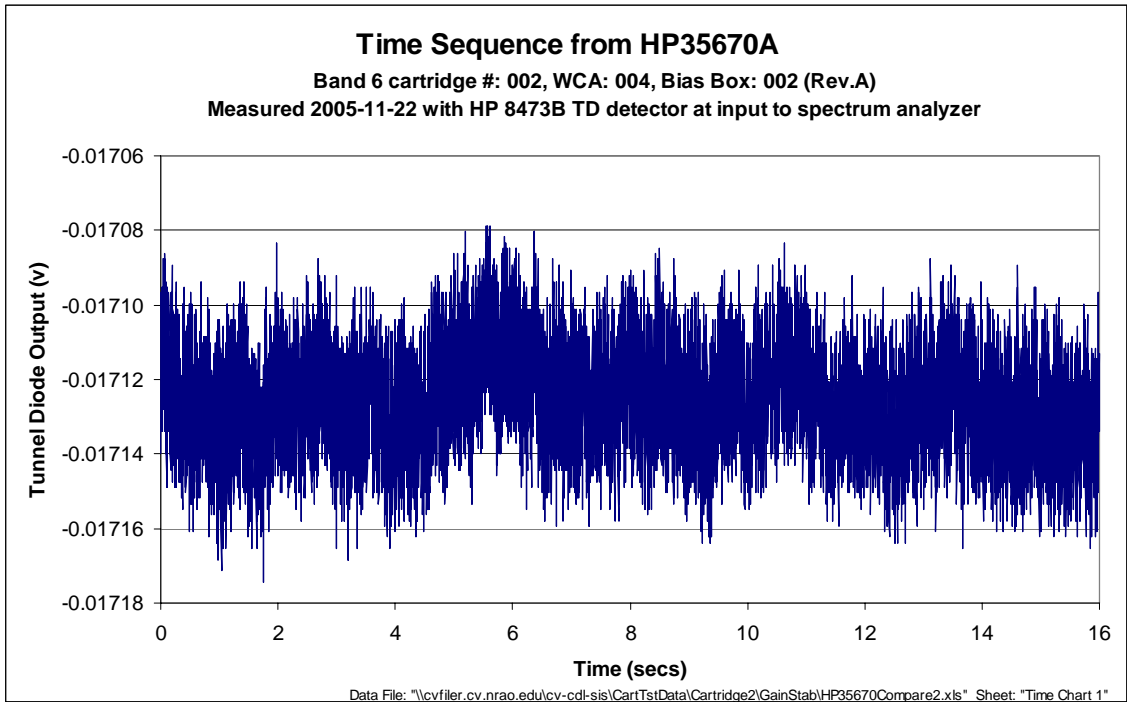


Figure 27: Time data from HP 35670A for 0.1 - 100 Hz Data in Figure 25

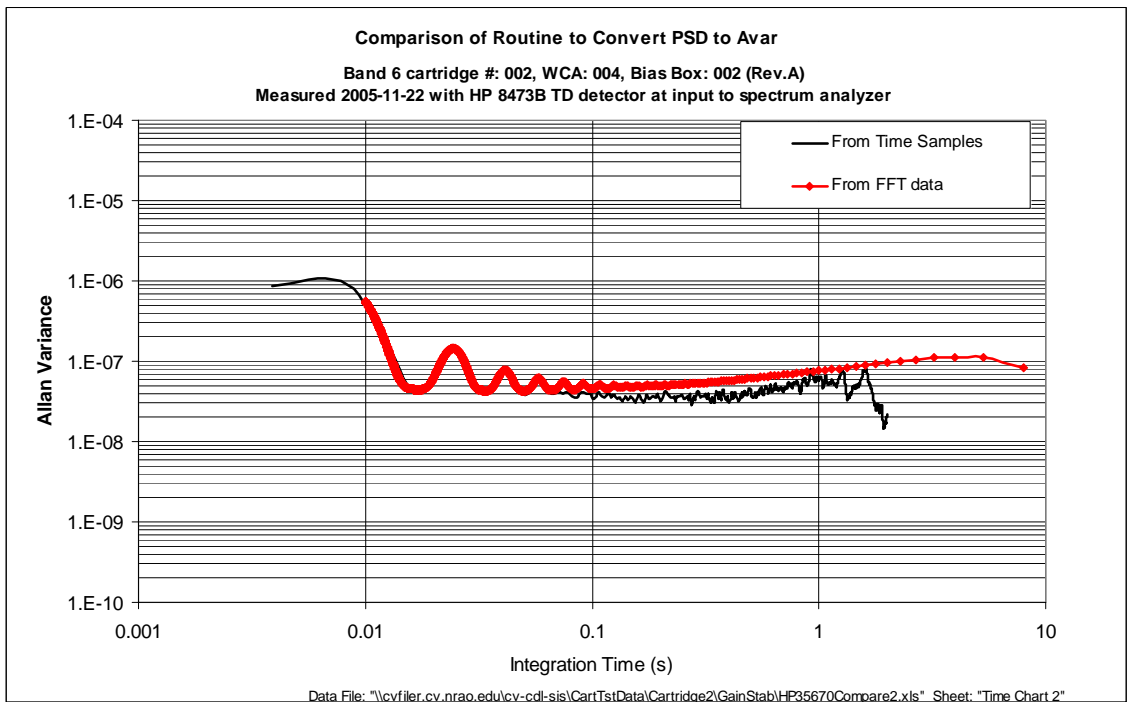
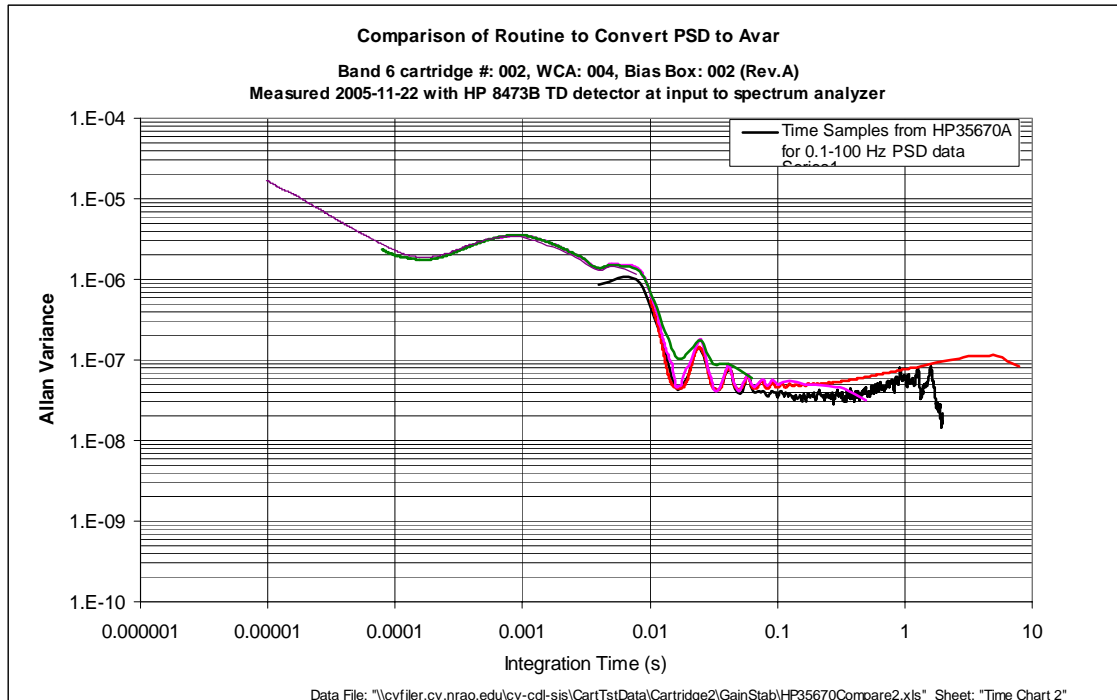


Figure 28: Comparison of AVAR Converted from from FFT and from Time Samples



**Figure 29: AVAR from PSD of Figure 25 and Time Data in Figure 27.
Compare to AVAR with superimposed sine wave, Figure 17**

5. References

- ^A “Band 6 Cartridge Technical Specifications,” FEND-40.02.06.00-001-A.04.SPE
- ^B David Allan, “Statistics for Atomic Frequency Standards,” IEEE Proc., Vol. 54, No. 2, February 1966.
- ^C The HP 35670A provides a scaled DC voltage in the zero-frequency bin, and that value is converted to average DC voltage by multiplying it by $\sqrt{F_{step}/2}$ where F_{step} is the FFT’s frequency step size.
- ^D E.J. Wollack and M.W. Pospieszalski, “Characteristics of Broadband InP Millimeter-Wave Amplifiers for Radiometry”, 1998, Proc. 1998 IEEE MTT-S Int. Microwave Symp. Digest, Baltimore, MD, pp 669-772 and also available as ALMA Memo 222 at <http://www.alma.nrao.edu/memos/html-memos/abstracts/abs222.html>.
- ^E J.A. Barnes, *et. al.*, “Characterization of Frequency Stability”, IEEE Trans. Instrum. Meas., Vol. IM-20, No. 2, pp. 105-120, May 1971. (Equation 72)
- ^F Characterization of Frequency and Phase Noise", Report 580, International Radio Consultative Committee (C.C.I.R.), pp. 142-150, 1986. (Equation 9)
- ^G B. Lazareff, “Allan variance derived from frequency domain measurements,” Unpublished note, E:\PCData\Rx\ALMA\Band7\Stability\PowerSpectrumToAllan.doc, 2004-05-04.